Journal of Modern Physics, 2017, 8, 1584-1606
http://www.scirp.org/journal/jmp
ISSN Online: 2153-120X
ISSN Print: 2153-1196

The Dissipative Flow in Topological Superconductors and Solid ^{4}He

D. Schmeltzer

Physics Department, City College of the City University of New York, New York, USA
Email: dschmeltzer@ccny.cuny.edu

How to cite this paper: Schmeltzer, D. (2017) The Dissipative Flow in Topological Superconductors and Solid ^{4}He. *Journal of Modern Physics*, **8**, 1584-1606.
https://doi.org/10.4236/jmp.2017.89095

Received: July 13, 2017
Accepted: August 25, 2017
Published: August 28, 2017

Abstract

Using two piezoelectric transducers, one measures the stress tensor response from the strain field generated by the second transducer. The ratio between the stress response and strain velocity determines the dissipative response. In the first part, we show that the dissipative stress response can be used for studying excitations in a topological superconductor. We investigate a topological superconductor for the case when an Abrikosov vortex lattice is formed. In this case, the Majorana fermions are dispersive, a fact that is used to compute the dissipative stress response. In the second part, we analyse the dissipative superfluid flow through solid ^{4}He discoused recently. We identify low energy, an excitation which plays the role of the Majorana mode which is free to move in a direction perpendicular to the two dimensional plane spaces of the dislocations.

Keywords

Topological Superconductor, Stress, Strain, Ultrasound, Solid ^{4}He

1. Introduction

The proximity of a superconductor [1] [2] to the surface of a topological insulator (TI) gives rise to a topological superconductor (TS) characterized by the Majorana zero modes. Recently, vortices and Majorana fermions in a magnetic field have been reported [3] in heterostructures of $Bi_2Te_3/NbSe_2$. Additionally, Majorana fermions have been studied in Abrikosov lattices [4] [5]. The Majorana zero modes are neutral excitations which, in an Abrikosov vortex lattice, become a gapless dispersive band [4] [5] [6]. In a variety of materials, a scanning tunneling microscope (STM) is used to detect charge tunneling.

A number of methods based on sound waves have been used to investigate superconductors [7] [8] [9] [10]. Ultrasound attenuation studies [11] [12], and investigations of the *p*-wave superconductor Sr_2RuO_2 have been carried out in ref. [13]. In the late fifties ultrasound attenuation techniques were used to measure the temperature dependence of the superconducting gap [14] [15] [16] [17] [18] and recently the techniques have been applied to liquid ^{3}He [19] and to ^{4}He by [20] where in the presence of a dislocation we have a direction where low energy excirtations are free to move in analogy with the Majoranas modes in topological superconductors.

The purpose of this paper is to demonstrate that piezoelectric transducers can be used to detect Majorana fermions in an Abrikosov vortex lattice and the dissipative flow trough ^{4}He can be explained.The tunneling amplitude of the Majorana fermions gives rise to a dispersive band [6] which is detectable. We compute the stress *viscosity* as a response to an applied strain velocity field [21] [22]. The explicit dependence of the strain field on the system is obtained from a coordinate transformation [23]. The linear stress response theory [24] used for a TS provides information about the Majorana fermions. In order to demonstrate the detection of Majorana fermions we consider a TS [1] [3] [4] [5] [25] [26] and consider the dissipative flow trough ^{4}He.

In this paper, we have derived the following specific results: (a) We have obtained the vortex lattice solution for a *p*-wave superconductor. (b) We have derived the stress-strain Hamiltonian and have computed the stress viscosity using the linear response theory. (c) We have identified the sound analog of the Andreev crossed reflection and have obtained the viscosity equivalent to the crossed reflection conductance. (d)We consider the analogues of the Majorana mode in solid ^{4}He.

The structure of the paper is as follows: In Section 2, we show that for an attractive interaction on the surface of a TI a TS is obtained. In the presence of an Abrikosov vortex lattice dispersive Majorana fermions are formed. In Section 3, we present the formation of the Abrikosov vortex lattice. We find dispersive Majorana fermions and quasi-particles in the vortex lattice. A new solution for the *p*-wave Abrikosov vortex lattice is obtained and discussed in detail. Section 4 is devoted to the derivation of the viscosity tensor for a TS. In Section 5, we compare our results to the one obtained by the ultrasound attenuation technique. In Section 6, we compute the transverse impedance for the TS in a magnetic field. The transverse impedance provides distinct information about the Abrikosov vortex lattice and the Majorana fermions. Our numerical estimates indicate that the signal should be experimentally detectable. Section 7 is devoted to studies of sound wave of the Andreev crossed reflection induced in one dimension by a piezoelectric transducer. In Section 8 we consider the disipative flow of a superfluid of ^{4}He through a solid ^{4}He [20]. Section 9 contains our main conclusions.

2. Formation of Majorana Fermions on the Surface of a TI with Attractive Interactions

In this section, we review the formation of a *p*-wave superconductor on the surface of a TI with attractive interactions. For two space dimensions, the quantum Hall system and the p-wave superconductor [1] [25] [26] are characterized by the first Chern integer number C^1 (which means that the integral of the Berry curvature over a closed manifold is quantized in units of 2π) [27]. In the presence of an attractive interaction (due to the electron-phonon interaction or proximity to another superconductor), on the surface of a TI a two-dimensional TS emerges. The proximity of a superconductor [1] to the three dimensional TI gives rise to Majorana zero modes on the surface of the TI. Recently it was reported that the application of a magnetic field on the heterostructure $Bi_2Te_3/NbSe_2$ induces an Abrikosov vortex lattice [3].

We propose that a realization of the model introduced in [1] emerges from the TI surface Hamiltonian $h(\boldsymbol{k}) = -\sigma_2 k_1 + \sigma_1 k_2$ in the presence of an attractive interaction. Here σ_1, σ_2 denote Pauli matrices and k_1, k_2 are wave vector components. We express the pairing interaction in terms of the field $\psi(\boldsymbol{x}) = \sum_k \mathrm{e}^{i\boldsymbol{k}\cdot\boldsymbol{x}} u^{(+)}(\boldsymbol{k})$ where $u^{(+)}(\boldsymbol{k})$ are the TI surface spinors for the conduction band, $u^{(+)}(\boldsymbol{k}) = \frac{1}{\sqrt{2}}\left[1, i\frac{k_1 - ik_2}{|\boldsymbol{k}|}\right]^{\mathrm{T}} \approx \frac{1}{\sqrt{2}}\left[1, i\frac{k_1 - ik_2}{k_0}\right]^{\mathrm{T}}$ (T stands for transpose), and k_0 is a momentum scale. This representation generates the linear derivatives of the pairing field. For a positive chemical potential $\mu > 0$ in the presence of a magnetic field, it gives rise to a superconductor with vortices. The attractive interaction expressed in terms of the TI spinors gives rise to the p-wave Hamiltonian [1] which in our case also includes vortices.

$$
\begin{aligned}
H_{T.I.+SC.} = \int \mathrm{d}^2 x \Bigg[& C^\dagger(\boldsymbol{x}) \frac{v}{2k_F}\left(\left(-i\partial_x - \frac{e}{\hbar}\boldsymbol{A}(\boldsymbol{x},t)\right)^2 - k_F^2\right) C(\boldsymbol{x}) \\
& + \frac{\Delta^*(\boldsymbol{x},t)}{2k_0} C(\boldsymbol{x},t)(\partial_1 - i\partial_2) C(\boldsymbol{x},t) \\
& - \frac{\Delta(\boldsymbol{x},t)}{2k_0} C^\dagger(\boldsymbol{x},t)(\partial_1 + i\partial_2) C^\dagger(\boldsymbol{x},t) + \frac{1}{g}|\Delta(\boldsymbol{x},t)|^2 \Bigg].
\end{aligned} \tag{1}
$$

Here $\boldsymbol{A}(\boldsymbol{x},t)$ is the vector potential and g is a coupling constant. The pairing field $\Delta(\boldsymbol{x})$ depends on the phase $\theta(\boldsymbol{x})$ which includes a multivalued part. We perform the gauge transformation: $C(\boldsymbol{x}) = \mathrm{e}^{\frac{-i}{2}\theta(\boldsymbol{x})}\hat{C}(\boldsymbol{x})$, $C^\dagger(\boldsymbol{x}) = \hat{C}^\dagger(\boldsymbol{x})\mathrm{e}^{\frac{i}{2}\theta(\boldsymbol{x})}$ and the Hamiltonian H is replaced by $\hat{H}$. The pairing field $\Delta(\boldsymbol{x})$ has points $\boldsymbol{x} \approx \boldsymbol{R}_k$, $k = 1, 2, \cdots$, where $\Delta(\boldsymbol{x})$ vanishes, $\Delta(\boldsymbol{x}) \approx |\Delta|\mathrm{e}^{i\theta(\boldsymbol{x})}$, $\Delta^\dagger(\boldsymbol{x}) = |\Delta|\mathrm{e}^{-i\theta(\boldsymbol{x})}$, where $\theta(\boldsymbol{x}) \equiv \theta(\boldsymbol{x}; \boldsymbol{R}_0 = 0, \boldsymbol{R}_1, \cdots, \boldsymbol{R}_k, \cdots)$ is the multivalued phase.

As a result of the gauge transformation the fermion operators $C(\boldsymbol{x})$, $C^\dagger(\boldsymbol{x})$ are replaced by $\hat{C}^\dagger(\boldsymbol{x})$, $\hat{C}(\boldsymbol{x})$ (and the Hamiltonian H is replaced by $\hat{H}$). The Hamiltonian $\hat{H}$ without the condensation energy $\frac{1}{g}|\Delta(\boldsymbol{x},t)|^2$ is expressed in terms of the particle-hole Pauli matrices τ_1, τ_2 and τ_3. We introduce the two-component spinor $\hat{\Psi}(\boldsymbol{x}) = \left[\hat{C}(\boldsymbol{x}), \hat{C}^\dagger(\boldsymbol{x})\right]^{\mathrm{T}}$ and find:

$$
\begin{aligned}
&\hat{H}=\int \mathrm{d}^2 x \hat{\Psi}^{\dagger}(\boldsymbol{x})\left[\tau_3 \hat{h}_3+\tau_2 \hat{h}_2+\tau_1 \hat{h}_1\right] \hat{\Psi}(\boldsymbol{x}), \\
&\frac{1}{2} \partial_x \theta(\boldsymbol{x}) \equiv \frac{1}{2} \sum_l \partial_x \varphi_l(\boldsymbol{x}), \ \varphi_l(\boldsymbol{x}) \equiv \arg\left(\boldsymbol{x}-\boldsymbol{R}_l\right), \\
&\hat{h}_3=\frac{v}{2 k_F}\left(\left(-i \partial_x-\frac{e}{\hbar} \boldsymbol{A}(\boldsymbol{x})+\frac{1}{2} \partial_x \theta(\boldsymbol{x})\right)^2-k_F^2\right), \\
&\hat{h}_2=i \frac{|\Delta(\boldsymbol{x})|}{2 k_0} \partial_1, \quad \hat{h}_1=-i \frac{|\Delta(\boldsymbol{x})|}{2 k_0} \partial_2 .
\end{aligned} \tag{2}
$$

The spinor $\hat{\Psi}(\boldsymbol{x})=\left[\hat{C}(\boldsymbol{x}),\hat{C}^{\dagger}(\boldsymbol{x})\right]^{\mathrm{T}}$ [28] contains two parts, the non-zero mode $\hat{\Psi}_{\neq 0}(\boldsymbol{x})$ and the zero mode (Majorana fermions) $\hat{\Psi}_0(\boldsymbol{x})$, $\hat{\Psi}(\boldsymbol{x}) \equiv \hat{\Psi}_{\neq 0}(\boldsymbol{x})+\hat{\Psi}_0(\boldsymbol{x})$.

3. TS Abrikosov Vortex Lattice

Next we discuss in detail the non-zero and zero modes of the Abrikosov lattice in a TS.

a) Non-zero modes

In this section we consider the non-zero modes for an Abrikosov vortex lattice in the presence of a magnetic field. The experimental work on the TS Bi_2Te_3/$NbSe_2$ [3] shows that an Abrikosov vortex lattice is formed. A vortex lattice is stabilized for superconductors when the penetration depth of the magnetic field is larger than the coherence length [15] [29]. We find for a single vortex a string-like solution for the effective magnetic field. For $|\hat{\boldsymbol{x}}|>d \approx \lambda_L$ the magnetic field vanishes (d is the vortex lattice constant and λ_L is the magnetic penetration depth). Since we are interested in the long distance behavior we can approximate the magnetic field for $|\boldsymbol{x}|<\lambda_L$ by a constant field, which is the spatial average around the vortex core with a radius of d.

Following refs. [15] [29] we solve the p-wave Hamiltonian in a periodic magnetic field b. The periodicity being $d \approx \lambda_L$. The periodic spinor solution is given by:

$W(\boldsymbol{x})=\sum_{n_2} \mathrm{e}^{iqn_2 y} f_{n_2}(x) W(x,n_2)$, where $f_{n_2}(x)=\mathrm{e}^{\frac{-b}{2}\left(x-\frac{q}{b}n_2\right)^2}$ and $W(x,n_2)=\left[U(x,n_2),V(x,n_2)\right]^{\mathrm{T}}$ is a two component spinor which is given by the eigenfunction of the p-wave Hamiltonian. We consider a square lattice and the solution is periodic in the y direction with the periodicity $d=d_y=\frac{2\pi}{q}$. The periodicity in the x direction $d=d_x=\frac{q}{b}$ is achieved by demanding the invariance of the Hamiltonian under the transformation, $n_2 \to n_2+1$. The system has a finite extention L in the x direction. Therefore the value of the momentum in the y direction must be restricted to $|n_2|<n_{\max}=\frac{bL}{q}=\frac{2L}{d}$ (to ensure that the states lie in the box $L \times L$).

Due to the spinor structure of the solution it is convenient to solve the problem in momentum space and at the end to impose the periodicity of the wave function. We represent the periodic solution as: $W(\boldsymbol{x})=\int\frac{\mathrm{d}^2k}{(2\pi)^2}\mathrm{e}^{i\boldsymbol{k}\cdot\boldsymbol{x}}W(\boldsymbol{k})$.

We use the momentum representation, $x=i\partial_{k_1}$ and find that for the *p*-wave Hamiltonian $h(\boldsymbol{k},i\partial_{k_1})$ in the magnetic field *b*:

$$h(\boldsymbol{k},i\partial_{k_1})=\tau_3\frac{v}{2k_F}\left[k_1^2+\left(k_2+ib\partial_{k_1}\right)^2-k_F^2\right]+\tau_1\frac{\Delta}{2k_0}k_2-\tau_2\frac{\Delta}{2k_0}k_1,$$

$$h(\boldsymbol{k},i\partial_{k_1})W(\boldsymbol{k})=E(\boldsymbol{k})W(\boldsymbol{k}), \tag{3}$$

where $bi\partial_{k_1}$ is the *y* component of the vector potential in the Landau gauge for the periodic magnetic field. The eigenvectors and eigenvalues are computed next. The ground state is given in terms of the ground state energy of the Harmonic oscillator solution, $\epsilon_0(b,k_F)\equiv\frac{vk_F}{2}\left(\sqrt{\frac{b^2}{2}}\right)$:

$$W(\boldsymbol{k})=\mathrm{e}^{i\frac{k_1k_2}{b}}\mathrm{e}^{-\frac{k_1^2\sqrt{2}}{b}}\hat{\hat{W}}(\boldsymbol{k}),$$

$$\hat{\hat{W}}(\boldsymbol{k})=\frac{1}{\sqrt{2}}\left[\mathrm{e}^{-i\chi(\boldsymbol{k})}\sqrt{1+\frac{\epsilon_0(b,k_F)}{E(\boldsymbol{k})}},\sqrt{1-\frac{\epsilon_0(b,k_F)}{E(\boldsymbol{k})}}\right]^{\mathrm{T}},$$

$$E(\boldsymbol{k})=\sqrt{\epsilon^2(b,k_F)+\left(\frac{\Delta}{2k_0}\right)^2\left(k_1^2+k_2^2\right)},$$

$$\epsilon_0(b,k_F)-\frac{v}{2k_F}k_F^2=\frac{vk_F}{2}\left(\frac{1}{2\pi}\frac{q^2}{k_F^2}-1\right). \tag{4}$$

We note that $\Delta/2k_0$ is dimensionless. At this stage we impose the periodic boundary conditions. This results in replacing $k_1=qn_1$, $k_2=qn_2$ with the condition $|n_2|<n_{\max}=\frac{bL}{q}=\frac{2L}{d}$, $q=\frac{2\pi}{d}$. As a result the eigenspinors and eigenvectors are given in terms of the integers n_1,n_2:

$$W(n_1,n_2)=\sqrt{\frac{1}{2n_{\max}+1}}\mathrm{e}^{i\frac{q^2n_1n_2}{b}}\mathrm{e}^{-\frac{q^2n_1^2\sqrt{2}}{b}}\hat{\hat{W}}(n_1,n_2),$$

$$\hat{\hat{W}}(n_1,n_2)=\frac{1}{\sqrt{2}}\left[\mathrm{e}^{-i\chi(n_1,n_2)}\sqrt{1+\frac{\epsilon(b,k_F)}{E(n_1,n_2)}},\sqrt{1-\frac{\epsilon(b,k_F)}{E(n_1,n_2)}}\right]^{\mathrm{T}}\equiv\left[U(n_1,n_2),V(n_1,n_2)\right],$$

$$E(n_1,n_2)=\sqrt{\epsilon^2(b,k_F)+\left(\frac{\Delta q}{2k_0}\right)^2\left(n_1^2+n_2^2\right)},\quad \epsilon(b,k_F)\equiv\frac{vk_F}{2}\left(\frac{q^2}{8\pi k_F^2}-1\right). \tag{5}$$

The spinor $W(n_1,n_2)$ determines the non-zero mode fermion fields. We introduce the annihilation and creation operators $\eta(n_1,n_2)$, $\eta^\dagger(n_1,n_2)$ with respect to the exact ground state $|G\rangle$, $\eta(n_1,n_2)|G\rangle=0$ which allows us to write:

$$\hat{\Psi}_{\neq 0}(\boldsymbol{x}) = \sum_{n_1}\sum_{n_2} \mathrm{e}^{iqn_1x_1 + i\frac{q}{2}n_2x_2}\left[\eta(n_1,n_2)W(n_1,n_2) + \eta^{\dagger}(-n_1,-n_2)\tau_1 \otimes IW^{*}(-n_1,-n_2)\right],$$

$$\hat{\Psi}^{\dagger}_{\neq 0}(\boldsymbol{x}) = \sum_{n_1}\sum_{n_2} \mathrm{e}^{-iqn_1x_1 - i\frac{q}{2}n_2x_2}\left[\eta^{\dagger}(n_1,n_2)W^{*}(n_1,n_2) + \eta(-n_1,-n_2)W(n_1,n_2)\tau_1 \otimes I\right]. \quad (6)$$

We have replaced the discrete sites by the coordinate x in order to consider even and odd rows that we need to introduce in the matrix I and double the dimension of the spinor. (This needs to be done in order to have the same dimension for the zero and nonzero modes). Taking in consideration also the particle-hole symmetry we use the representation $\tau_1 \otimes I$, which is four-dimensional; τ_1 acts on the particle-hole space and $I = 1,2$ acts on the even and odd row in real space.

b) Zero modes

In this section we consider the zero modes for an Abrikosov vortex lattice. In the absence of the vortex lattice the zero-mode solutions for the Hamiltonian in Equation (2) are given by:

$W_0(\boldsymbol{x}) \equiv W_0(r,\varphi) = \left[U_0(r,\varphi), V_0(r,\varphi)\right]^{\mathrm{T}} \equiv \left[\frac{1}{\sqrt{i}}\mathrm{e}^{\frac{i}{2}\varphi}, \frac{1}{\sqrt{-i}}\mathrm{e}^{\frac{-i}{2}\varphi}\right]^{\mathrm{T}} \frac{F(r)}{\sqrt{r}}$. The function $\frac{F(r)}{\sqrt{r}}$ obeys the normalization condition $\int \mathrm{d}^2 r\left[\frac{F(r)}{\sqrt{r}}\right]^2 < \infty$. Due to the charge conjugation property of the Hamiltonian, the zero modes are Majorana modes. The solution obtained here is similar to the solution given in refs. [27] [30] for the p-wave superconductors. The explicit form of the kinetic operator determines the exact form of the amplitude $\frac{F(r)}{\sqrt{r}}$ for the zero modes [31]. We consider the case where the gauge transformed Hamiltonian $\hat{H}$ has $2N$ Majorana zero modes. The Majorana operators obey $\gamma_l = \gamma_l^{\dagger}$, $\gamma_l^2 = \frac{1}{2}$ for $l = 1, \cdots, 2N$,

$$\hat{\Psi}_0(\boldsymbol{x}) = \sum_{l=1}^{2N} \gamma_l \left[\frac{1}{\sqrt{i}}\mathrm{e}^{\frac{i}{2}\varphi_l(x)}, \frac{1}{\sqrt{-i}}\mathrm{e}^{\frac{-i}{2}\varphi_l(x)}\right]^{\mathrm{T}} \frac{F(|\boldsymbol{x}-\boldsymbol{R}_l|)}{\sqrt{|\boldsymbol{x}-\boldsymbol{R}_l|}}. \quad (7)$$

In the second stage we want to discuss the effect of the vortex lattice on the localized Majorana fermions. The effect of the vortex lattice is to delocalize the Majorana fermions and form dispersive Majorana bands. This is a result due to ref. [4] which showed that Majorana fermions enclose a flux which depends on the number of vortices on a closed polygon. The flux on a polygon of n vortices is $\frac{\pi}{2}(n-2)$ (n is the number of vortices in the polygon) [4]. For a square vortex lattice with four vortices ($n = 4$) per plaquette the flux will be $\frac{\pi}{2}(4-2) = \pi$. For the Majorana case we restrict ourselves to plaquettes with four vortices (per plaquette) [4]. We consider the effect of the overlap between Majorana fermions given by matrix element t_0 [4] [6].

$$H_0 = it_0 \sum_{i,j} \hat{\Psi}_0^\dagger(x_i) S(x_i, x_j) \hat{\Psi}_0(x_j), \tag{8}$$

where $S(x_i, x_j)$ introduces the phase on the bond i, j and determines the flux of π per plaquette and t_0 is the overlap between the Majorana fermions which is determined from Eqution (7). (The minimum energy for the Abrikosov vortices is obtained for a triangular lattice [29]. For a square lattice the energy is less favorable, but it is simpler to analyze.)

We choose a gauge for which the hopping constant along columns has positive sign and alternating signs between adjacent rows. This means that $S(x_i, x_j) = |S(x_i, x_j)| \mathrm{e}^{i\theta_{i,j}}$, the phase $\theta_{i,j}$ is zero along columns, has positive sign ($\theta_{i,j} = 0$) and alternating signs between adjacent rows ($\theta_{i,j} = \pi$) [4]. As a result we obtain two flat bands and a third band that is dispersive and gapless [4] [5] [6] comprising Majorana fermions with the eigenvalues:

$$\lambda_{\alpha=1}^0(\boldsymbol{k}) \equiv \lambda(\boldsymbol{k}) = t_0 \sqrt{\sin^2(k_1) + \sin^2(k_2)}, \quad |\boldsymbol{k}| \le \frac{\pi}{2}, \quad \lambda_{\alpha=2}^0(\boldsymbol{k}) = 0. \tag{9}$$

For the zero modes we find that the representation of the zero modes is given in terms of the zero mode Majorana operators in the continuum representation $\Gamma(\boldsymbol{x}) = \Gamma^\dagger(\boldsymbol{x})$ (x_i is replaced with the continuum coordinate *x*, even and odd rows are introduced with the help of the matrix I) and spinor eigenfunctions are given in momentum space $L(\boldsymbol{k})$:

$$\begin{aligned} \hat{\Psi}_0(\boldsymbol{x}) &= \sum_k \mathrm{e}^{i\boldsymbol{k}\cdot\boldsymbol{x}} \left[\Gamma(\boldsymbol{k}) L(\boldsymbol{k}) + \Gamma^\dagger(-\boldsymbol{k}) \tau_1 \otimes I L^*(-\boldsymbol{k}) \right], \\ \hat{\Psi}_0^\dagger(\boldsymbol{x}) &= \sum_k \mathrm{e}^{-i\boldsymbol{k}\cdot\boldsymbol{x}} \left[\Gamma^\dagger(\boldsymbol{k}) L^*(\boldsymbol{k}) + \Gamma(-\boldsymbol{k}) L(-\boldsymbol{k}) \tau_1 \otimes I \right]. \end{aligned} \tag{10}$$

The four components of the spinor $L(\boldsymbol{k})$ in Equation (10) are given by:

$$L(\boldsymbol{k}) = \frac{1}{\sqrt{2}\sqrt{\sin^2[k_1] + 4(\sin[k_1] + \lambda(\boldsymbol{k}))^2}}$$

$$\left[\sin[k_2], \sin[k_2], \frac{-i(\sin[k_1] + \lambda(\boldsymbol{k}))}{\sin[k_2]} (1 - \mathrm{e}^{2ik_2}), \frac{-i(\sin[k_1] + \lambda(\boldsymbol{k}))}{\sin[k_2]} (1 - \mathrm{e}^{2ik_2}) \right]^{\mathrm{T}}. \tag{11}$$

We replace the discrete sites x_i by the coordinate *x*, therefore we introduce the matrix I to double the dimension of the spinor. Taking in consideration also the particle-hole symmetry we use the representation $\tau_1 \otimes I$ which is four-dimensional; τ_1 acts on the particle-hole space and $I = 1, 2$ acts on the even and odd row. We note that a triangular lattice for the Majorana modes has been considered in refs. [4] [6].

4. Viscosity Tensor for the Topological Superconductor

In this section we introduce the theory for the dissipative viscosity. In Sec. V and Sec. VI we use this theory to investigate the Abrikosov lattice. The physics of solids [21] and fluids [22] provides us the relation between the stress tensor Σ_{ij}, strain field ϵ_{kl} and the velocity strain field $v_{kl}=\partial_t(\epsilon_{kl})$ [32]. We now use this description for quantum fluids in a solid. The combination of the stress tensor resulting from a strain field and the dissipative part of the stress determines the equation:

$$\Sigma_{ij}=\lambda_{ij,kl}\epsilon_{kl}+\zeta_{ij,kl}v_{kl}. \tag{12}$$

The strain field $\epsilon_{k,l}$ is given in terms of the lattice deformation $\boldsymbol{u}(\boldsymbol{x},t)$, $\epsilon_{k,l}=\frac{1}{2}\left(\partial_k u^l+\partial_l u^k\right)$, $\epsilon_{0,i}=\partial_t u^i$. The viscosity tensor is given by $\zeta_{ij,kl}\equiv\frac{\Sigma_{ij}}{v_{kl}}$, and $\zeta_{ij,kl}$ is separated into two parts, $\zeta_{ij,kl}=\zeta^S_{ij,kl}+\zeta^A_{ij,kl}$, $\zeta^S_{ij,kl}=\zeta^S_{kl,ij}$ is the symmetric part and $\zeta^A_{ij,kl}=-\zeta^A_{kl,ij}$ is the antisymmetric part [33]. From the Onsager relations [34] we know that when the time reversal symmetry is violated, like in the quantum Hall system and the *p*-wave superconductor case [26] [33] [35] [36], we have $\zeta^A_{ij,kl}\neq 0$. For $\zeta_{ii,kk}$ with $i\neq k$ we have a situation where the strain field generates stress in the perpendicular direction. The stress tensor for quantum fluids is obtained from the invariance of the Lagrangian under an arbitrary local coordinate transformation [23] [37] [38] [39]. The explicit dependence of the strain field on the lattice deformation determines the coordinate transformation [23] from which we obtain the stress tensor. In the presence of an elastic deformation $\boldsymbol{u}$ the coordinates transform in the following way: $\boldsymbol{x}\to\boldsymbol{\xi}(\boldsymbol{x})=\boldsymbol{x}+\boldsymbol{u}(\boldsymbol{\xi})$ [23] (see the **Appendix**).

This coordinate transformation allows the identification of the stress tensor. Using the invariance of the *spinless* fields under the coordinate deformation gives,

$$\hat{\mathbf{C}}(\boldsymbol{\xi}(\boldsymbol{x}))=\hat{C}(\boldsymbol{x}),\quad \hat{\mathbf{C}}^\dagger(\boldsymbol{\xi}(\boldsymbol{x}))=\hat{C}^\dagger(\boldsymbol{x}). \tag{13}$$

For the *p*-wave Hamiltonian given in Equation (2) we find the momentum density $\pi_i(\boldsymbol{x},t)$ and stress tensor $\Sigma_{ij}(\boldsymbol{x},t)$ induced by the strain fields $\epsilon_{0i}(\boldsymbol{x},t)$, $\epsilon_{ij}(\boldsymbol{x},t)$. To linear order in the deformation strain field we obtain the response stress field. Using the invariance, Equation (13), with respect to the coordinate transformation determines the strain-stress Hamiltonian $H^{ext}(t)$:

$$\begin{aligned}H^{ext}(t)=\int\mathrm{d}^2x\big[&\epsilon_{01}(\boldsymbol{x},t)\pi_1(\boldsymbol{x},t)+\epsilon_{02}(\boldsymbol{x},t)\pi_2(\boldsymbol{x},t)+\epsilon_{11}(\boldsymbol{x},t)\Sigma_{11}(\boldsymbol{x},t)\\&+\epsilon_{22}(\boldsymbol{x},t)\Sigma_{22}(\boldsymbol{x},t)+\epsilon_{12}(\boldsymbol{x},t)\Sigma_{12}(\boldsymbol{x},t)+\Omega_{12}(\boldsymbol{x},t)R_{12}(\boldsymbol{x},t)\big].\end{aligned} \tag{14}$$

In the absence of disclinations $\Omega_{12}(\boldsymbol{x},t)=0$ in Equation (14).

Using the explicit dependence of the spinor in Equation (2) allows us to represent the stress fields:

$$\pi_1(\boldsymbol{x},t)=\hat{\Psi}^\dagger(\boldsymbol{x},t)(Ii\partial_1)\hat{\Psi}(\boldsymbol{x},t);\quad \pi_2(\boldsymbol{x},t)=\hat{\Psi}^\dagger(\boldsymbol{x},t)(Ii\partial_2)\hat{\Psi}(\boldsymbol{x},t),$$

$$\Sigma_{11}(\boldsymbol{x},t)\approx-\frac{\Delta}{2k_0}\hat{\Psi}^\dagger(\boldsymbol{x},t)\left(\tau_2(-\partial_1)\hat{\Psi}(\boldsymbol{x},t)\right);$$

$$\Sigma_{22}(\boldsymbol{x},t)\approx-\frac{\Delta}{2k_0}\hat{\Psi}^\dagger(\boldsymbol{x},t)\left(\tau_1(-i\partial_2)\right)\hat{\Psi}(\boldsymbol{x},t),$$

$$\Sigma_{12}(\boldsymbol{x},t)\approx\frac{\Delta}{2k_0}\hat{\Psi}^\dagger(\boldsymbol{x},t)\left(\tau_2(-i\partial_2)+\tau_1(-i\partial_1)\right)\hat{\Psi}(\boldsymbol{x},t);$$

$$R_{12}(\boldsymbol{x},t) \approx \frac{\Delta}{2k_0} \hat{\Psi}^{\dagger}(\boldsymbol{x},t)\left(\tau_2(-i\partial_2) - \tau_1(-i\partial_1)\right)\hat{\Psi}(\boldsymbol{x},t);\ \hat{\Psi}(\boldsymbol{x}) \equiv \hat{\Psi}_{\neq 0}(\boldsymbol{x}) + \hat{\Psi}_0(\boldsymbol{x}). \quad (15)$$

We compute the viscosity stress tensor and the *dissipative* viscosity tensor $\zeta_{ij,kl}(\boldsymbol{q},\Omega) = \frac{\Sigma_{ij}(\boldsymbol{q},\Omega)}{v_{kl}(-\boldsymbol{q},-\Omega)}$ in quantum fluids. We vary the *p*-wave Hamiltonian by a linear strain field $\delta u^i(\boldsymbol{x},t)$, $u^i(\boldsymbol{x},t) \to u^i(\boldsymbol{x},t) + \delta u^i(\boldsymbol{x},t)$ and find from Equation (6) that the variation with respect to $\delta u^i(\boldsymbol{x},t)$ satisfies the continuity equation:

$$\partial_t \pi_j(\boldsymbol{x},t) + \sum_i \partial_i \Sigma_{ij}(\boldsymbol{x},t) = 0. \quad (16)$$

Using the linear response theory [24] with respect to the strain-stress Hamiltonian $H^{ext}(t)$ given in Equation (14) we obtain:

$$\langle G|\Sigma_{ij}(x,t)|G\rangle_{ext} = \langle G|\Sigma_{ij}(x,t)|G\rangle + \left(\frac{-i}{\hbar}\right)\int_0^t \mathrm{d}t' \langle G|\left[\Sigma_{ij}^H(x,t), H_H^{ext}(t')\right]|G\rangle, \quad (17)$$

where $\Sigma_{ij}^H(x,t)$ is the stress in the Heisenberg representation computed with respect the ground state $|G\rangle$ of the Hamiltonian in Equation (2). Following ref. [24] we obtain the relation $\Sigma_{ij}(\boldsymbol{q},\Omega) = \zeta_{ij,kl}(\boldsymbol{q},\Omega) v_{kl}(-\boldsymbol{q},-\Omega)$:

$$R_{ij,kl}(\boldsymbol{q},t) = \left(\frac{-i}{\hbar}\right)\langle G|\mathbf{T}\left(\Sigma_{ij}(\boldsymbol{q},t)\Sigma_{kl}(-\boldsymbol{q},0)\right)|G\rangle,$$

$$R_{ij,kl}(\boldsymbol{q},\Omega) = \int_{-\infty}^{\infty} R_{ij,kl}(\boldsymbol{q},t)\mathrm{e}^{-i\Omega t}\mathrm{d}t,$$

$$\zeta_{ij,kl}(\boldsymbol{q},\Omega) = -\frac{R_{ij,kl}(\boldsymbol{q},\Omega)}{i\Omega}. \quad (18)$$

The *dissipative* $\zeta_{ij,kl}(\boldsymbol{q},\Omega)$ part of the viscosity tensor is obtained after the analytic continuation $i\Omega \to \Omega + i0^+$. Equation (18) is computed using Wick's theorem [24] for the stress $\Sigma_{ij}(\boldsymbol{q},t)$ which is expressed in terms of the spinor $\hat{\Psi}(\boldsymbol{x}) = \hat{\Psi}_{\neq 0}(\boldsymbol{x}) + \hat{\Psi}_0(\boldsymbol{x})$ in Equation (15).

5. Application of the Viscosity Tensor to Ultrasound Attenuation

In this section we compare our calculation to the existing ultrasound attenuation method given in the literature [14] [15] [16]. For the topological superconductors we need to work with the spinor $\hat{\Psi}(\boldsymbol{x}) = \hat{\Psi}_{\neq 0}(\boldsymbol{x}) + \hat{\Psi}_0(\boldsymbol{x})$. Due to the dispersive nature of the zero modes, we will have new contributions to the absorption from the mixed pairs $\hat{\Psi}_{\neq 0}(\boldsymbol{x})$ and $\hat{\Psi}_0(\boldsymbol{x})$.

In a superconductor the electron-phonon interaction couples to longitudinal as well as transverse phonons. The coupling of the electrons to the transverse phonons in the superconducting phase is less understood. We show that by applying a transverse strain we can obtain non-diagonal response for stress; in this way we study the transverse effect of phonons.

The ultrasound attenuation method measures the superconducting gap. The single particle contribution to the absorption in a superconductor is given by

$\frac{\alpha_{sc}}{\alpha_{\text{normal}}}=\frac{2}{e^{\frac{\Delta(T)}{T}}+1}$ (α_{sc} is the absorption for the superconductor and α_{normal} is the absorption in the normal phase). In our case we have contributions from the electrons and the Majorana modes. Due to the magnetic vortex lattice the absorption is given by discrete summations instead of the integration of quasi-particle density of states. The absorption of transverse phonons is obtained from the response of non-diagonal strain tensor $\epsilon_{ij}(\boldsymbol{x},t)$. Theoretically we express the strain tensor $\epsilon_{ij}(\boldsymbol{x},t)$ in terms of the normal modes of the harmonic crystal [32] [$\epsilon_{ij}(\boldsymbol{x},t)$ depends only on the crystal phonons] without requiring knowledge of the explicit electron-phonon interaction. The strain tensor $\epsilon_{ij}(\boldsymbol{x},t)$ is represented in terms of the normal phonon operators $b_s(\boldsymbol{Q})$ and $b_s^{\dagger}(\boldsymbol{Q})$ ($s=1,2$ are the two phonon polarizations for a phonon in the i direction given by the vector $\boldsymbol{e}$ in the orthogonal direction to the vector $\boldsymbol{Q}$):

$$\varepsilon_{ij}(-\boldsymbol{Q},t)=\sum_{s}\frac{1}{2\pi}\sqrt{\frac{\hbar}{2\rho}}\frac{1}{\sqrt{\omega_s(\boldsymbol{Q})}}\left[ie_s^{(i)}(\boldsymbol{Q})Q_j\left(b_s^{\dagger}(\boldsymbol{Q})+b_s(-\boldsymbol{Q})\right)\right]. \tag{19}$$

In order to compute the dissipation for the vortex lattice Hamiltonian with the eigenvalues and wave function given in Equation ((5), (6)) stress-strain Hamiltonian (the representation of the Hamiltonian in Equation (14)). We need to do it for the non-zero mode part and zero mode. For the non zero mode we have from Equation (5) the representation, $H^{\neq 0}=\int \mathrm{d}^2x\hat{\Psi}^{\dagger}_{\neq 0}(\boldsymbol{x})E(\boldsymbol{x})\hat{\Psi}_{\neq 0}(\boldsymbol{x})$

Where $E(\boldsymbol{x})$ is the real space representation of $E(\boldsymbol{k})$ given in Equation (4). Next we use the invariance of the spinors under the coordinates transformation following Equation (13) and the metric transformation given by the Jacobian transformation given in **Appendix** we obtain the the stress-strain coupling for the non-zero modes. We perform a similar derivation for the zero mode part.

As a result we find to lowest order the strain stress Hamiltonian:

$$\begin{aligned}H^{ext}(t)=\int \mathrm{d}^2x\Big[&\left(\epsilon_{11}(\boldsymbol{x})+\epsilon_{22}(\boldsymbol{x})\right)\hat{\Psi}^{\dagger}_{\neq 0}(\boldsymbol{x})E(0)\hat{\Psi}_{\neq 0}(\boldsymbol{x})+\epsilon_{11}(\boldsymbol{x})t_0\Big(\hat{\Psi}^{\dagger}_0(\boldsymbol{x})\hat{\Psi}_0(\boldsymbol{x})\\&+\hat{\Psi}^{\dagger}_0(\boldsymbol{x})\partial_1\hat{\Psi}_0(\boldsymbol{x})\Big)+\epsilon_{22}(\boldsymbol{x})t_0\left(\hat{\Psi}^{\dagger}_0(\boldsymbol{x})\hat{\Psi}_0(\boldsymbol{x})+\hat{\Psi}^{\dagger}_0(\boldsymbol{x})\partial_2\hat{\Psi}_0(\boldsymbol{x})\right)\\&+\epsilon_{12}(\boldsymbol{x})t_0\hat{\Psi}^{\dagger}_0(\boldsymbol{x})\partial_1\hat{\Psi}_0(\boldsymbol{x})+\epsilon_{21}(\boldsymbol{x})t_0\hat{\Psi}^{\dagger}_0(\boldsymbol{x})\partial_2\hat{\Psi}_0(\boldsymbol{x})\Big]\end{aligned}$$

The contribution to the stress-strain Hamiltonian for the no-zero modes is given by the change of the metric given by the Jacobian of the coordinate transformation **e** (see the **Appendix**). For the zero mode we have two contribution one from the metric change **e** and the first order derivative originates from the Fourier tranform of the eigenvalue $\lambda_1^0(\boldsymbol{k})$. This will be our new stress-strain Hamitonian which replaces Equation (15).

Using first order perturbation theory we compute the ultrasound attenuation in agreement with refs. [14] [15] [16].

Following ref. [21], the transverse sound absorption $\alpha_t(\Omega)$ and longitudinal absorption $\alpha_t(\Omega)$ can be represented in terms of the viscosity tensor

$\zeta_{12,12}(\boldsymbol{q},\Omega)$ and $\zeta_{11,11}(\boldsymbol{q},\Omega)$ defined in Equation (18). In two dimensions we have for the transverse absorption, $\alpha_t(\Omega)=\zeta^{\perp}(\Omega)\frac{\Omega^2}{2\rho v_{s,\perp}^3}$ where $\zeta^{\perp}(\Omega)=\frac{1}{2}\left(\zeta_{12,12}(\Omega)+\zeta_{21,21}(\Omega)\right)$. The longitudinal absorption is given by $\alpha_l(\Omega)=\zeta^{\parallel}(\Omega)\frac{\Omega^2}{2\rho v_{s,\parallel}^3}$ where $\zeta^{\parallel}(\Omega)=\frac{1}{2}\left(\zeta_{11,11}(\Omega)+\zeta_{22,22}(\Omega)\right)$. The information about the crystal enters through the sound velocity $v_{s,\perp}$ (transverse), $v_{s,\parallel}$ (longitudinal), crystal density ρ and quantum fluid viscosity $\zeta_{ij,kl}(\boldsymbol{q},\Omega)$. For example the viscosity terms $\zeta_{11,11}(\boldsymbol{q},\Omega)$ are computed according to Equation (18) using the mode expansion of the spinor $\hat{\Psi}(\boldsymbol{x})=\hat{\Psi}_{\neq 0}(\boldsymbol{x})+\hat{\Psi}_0(\boldsymbol{x})$ which allows us to compute the longitudinal absorption: $R_{\parallel,\parallel}^{\neq 0,\neq 0}(\boldsymbol{Q},t)$ represents the non-zero mode part [the index $\neq 0,\neq 0$ means that the two fields which contribute to absorption are only non-zero modes, the symbol $\parallel,\parallel$ means that we have contributions only from $\zeta_{11,11}(\Omega)$ and $\zeta_{22,22}(\Omega)$]. Similarly, $R^{\neq 0,0}(\boldsymbol{Q},t)$ represents the mixed contribution, a zero mode and a non-zero mode (one field contains the zero mode and the second contains the non-zero mode) whereas $R^{0,0}(\boldsymbol{Q},t)$ represents the contribution when both fields are zero modes.

Using the imaginary time order operator T_t in the imaginary time representation [24] we find: for $i=2$ the tensor $R_{22,22}(\boldsymbol{Q},t)$ is given as
$R_{22,22}(\boldsymbol{Q},t)=-T_t\langle G|\Sigma_{22}(\boldsymbol{Q},t)\Sigma_{22}(-\boldsymbol{Q},t)|G\rangle$, and
$R_{22,22}(\boldsymbol{Q},t)=R_{22,22}^{\neq 0,\neq 0}(\boldsymbol{Q},t)+R_{22,22}^{\neq 0,0}(\boldsymbol{Q},t)+R_{22,22}^{0,0}(\boldsymbol{Q},t)$.

The *particle-hole* contribution is given by $R_{22,22}^{\neq 0,\neq 0}(\boldsymbol{Q},t;qp)$ (the particle-particle contributions are neglected and the symbol qp means particle-hole). The mixed terms particle-Majorana and hole-Majorana are given by $R^{\neq 0,0}(\boldsymbol{Q},t;qp)$. Using Wick's theorem with the spinor representation given in Equation ((5), (10)) we compute $R_{22,22}(\boldsymbol{Q},t)$ and $\zeta_{22,22}(\boldsymbol{Q},\Omega)$.

a) Non-zero modes absorption

We consider first the absorption for the particle-hole in the absence of Majorana modes. We find for the dissipative viscosity $\zeta_{22,22}^{\neq 0,\neq 0}(\boldsymbol{Q},\Omega;qp)$:

$$\zeta_{22,22}^{\neq 0,\neq 0}(\boldsymbol{Q},\Omega;qp)=\left(\frac{\Delta}{k_0}\right)^2\left[\frac{1}{2}k_F^2+Q_2^2\right]\sum_{n_1}\sum_{n_2}\left[\frac{1}{\mathrm{e}^{\frac{E(n_1,n_2)}{T}}+1}-\frac{1}{\mathrm{e}^{\frac{E\left(n_1,n_2-\frac{Q_2 d}{2\pi}\right)}{T}}+1}\right]$$
$$\times\left(\frac{-i}{\Omega}\right)\left[\frac{1}{i\hat{\Gamma}+\Omega+E(n_1,n_2)-E\left(n_1,n_2-\frac{Q_2 d}{2\pi}\right)}-\frac{1}{i\hat{\Gamma}+\Omega-E(n_1,n_2)+E\left(n_1,n_2-\frac{Q_2 d}{2\pi}\right)}\right], \tag{20}$$

where $E(n_1,n_2)$ is the quasi-particle dispersion given in Equation (11). Here $\hat{\Gamma}$ denotes the scattering life-time for the quasi-particles, d is the lattice separation between the vortices, Ω is the frequency of the transducer strain field and T is the temperature.

For an *s*-wave superconductor the absorption agrees with the results given in the literature, $\frac{\alpha_{sc}}{\alpha_{\text{normal}}}=\frac{2}{\mathrm{e}^{\frac{\Delta(T)}{T}}+1}$. For the present case with the dispersion $E(n_1,n_2)$, the absorption is controlled by the magnetic field with the ground state energy $\epsilon(b,k_F)$ [see Equation (11)].

b) Absorption due to Majorana modes

The Majorana modes give rise to the particle-hole (Majorana) absorption $\zeta_{22,22}^{\neq 0,0}(\boldsymbol{Q},\Omega;qp)$ and the particle-particle (Majorana) absorption $\zeta_{22,22}^{\neq 0,0}(\boldsymbol{Q},\Omega;qp)$. This notation means that the absorption is controlled by a zero and a non-zero mode, "$0,\neq 0$" and the non-zero mode is either a particle-hole "qp" or a particle-particle "pp" channel. Both absorptions are controlled by the tunneling amplitude t_0 of the dispersive Majorana mode. From the particle-hole (Majorana) absorption $\zeta_{22,22}^{\neq 0,0}(\boldsymbol{Q},\Omega;qp)$ we have the combination where the nonzero mode is a particle and the Majorana operator in the fermionic representation Γ [see Equation (5)] is a hole or *vice versa*. We introduce the scattering life time ($\hat{\Gamma}$) and find for $\zeta_{22,22}^{\neq 0,0}(\boldsymbol{Q},\Omega;qp)$ the representation:

$$\zeta_{22,22}^{\neq 0,0}(\boldsymbol{Q},\Omega;qp)=\left(\frac{\Delta}{k_0}\right)^2\left[\frac{1}{2}k_F^2+Q_2^2\right]\sum_{n_1}\sum_{n_2}\left[\frac{1}{\mathrm{e}^{\frac{\lambda(n_1,n_2)}{T}}+1}-\frac{1}{\mathrm{e}^{\frac{E\left(n_1,n_2-\frac{Q_2 d}{2\pi}\right)}{T}}+1}\right]$$
$$\times\left(\frac{-i}{\Omega}\right)\left[\frac{1}{i\hat{\Gamma}+\Omega+\lambda(n_1,n_2)-E\left(n_1,n_2-\frac{Q_2 d}{2\pi}\right)}-\frac{1}{i\hat{\Gamma}+\Omega-\lambda(n_1,n_2)+E\left(n_1,n_2-\frac{Q_2 d}{2\pi}\right)}\right], \tag{21}$$

where $\lambda(n_1,n_2)$ is the dispersion of the Majorana fermions given in Equation (4).

The particle-particle (Majorana) absorption (this is the case that a non-zero mode particle and a zero mode Majorana are created) $\zeta_{22,22}^{\neq 0,0}(\boldsymbol{Q},\Omega;pp)$ is given by:

$$\zeta_{22,22}^{\neq 0,0}(\boldsymbol{Q},\Omega;pp)=\left(\frac{\Delta}{k_0}\right)^2\left[\frac{1}{2}k_F^2+Q_2^2\right]\sum_{n_1}\sum_{n_2}\left[1-\frac{1}{\mathrm{e}^{\frac{\lambda(n_1,n_2)}{T}}+1}-\frac{1}{\mathrm{e}^{\frac{E\left(n_1,n_2-\frac{Q_2 d}{2\pi}\right)}{T}}+1}\right]$$
$$\times\left(\frac{\Gamma}{\Omega}\right)\left[\frac{1}{\left(\Omega-\lambda(n_1,n_2)-E\left(n_1,n_2-\frac{Q_2 d}{2\pi}\right)\right)^2+\hat{\Gamma}^2}\right], \tag{22}$$

where $\lambda(n_1,n_2)$ is the dispersion of the Majorana fermions given in Equation (4). From the theory of electromagnetic paramagnetic response in superconductors [see ref. [14], Equations (8.47)-(8.50)] we can see the similarity with our results, Equations ((21), (22)). In our case the electric field is replaced by the strain velocity $\partial_t \epsilon_{k,l}$.

6. Transverse Impedance for Topological Superconductors

The transverse impedance $\zeta_{22,01}(\boldsymbol{Q},\Omega;)$ is given by: $\zeta_{22,01}(\boldsymbol{Q},t)=\dfrac{\Sigma_{22}(\boldsymbol{Q},\Omega)}{\partial_t u^1(t)}$.

It describes the response of the stress field in the $i=2$ direction to an applied strain field in the $i=1$ direction similar to the Hall effect. In the frequency space we have:

$$\Sigma_{22}(\boldsymbol{Q},\Omega)=\left[\frac{\lambda_{22,01}}{i\Omega}+\zeta_{22,01}(\boldsymbol{Q},\Omega)\right]v_1(\Omega),\quad v_1(\Omega)=-i\Omega u^1(\Omega),$$
$$\zeta_{22,01}(\boldsymbol{Q},\Omega)\equiv\zeta^R_{22,01}(\boldsymbol{Q},\Omega)+i\zeta^I_{22,01}(\boldsymbol{Q},\Omega),\tag{23}$$

where $\zeta^R_{22,01}(\boldsymbol{Q},\Omega)$ is the real dissipative part and $i\zeta^I_{22,01}(\boldsymbol{Q},\Omega)$ is the imaginary part. We now compute the transverse impedance for the TS Abrikosov vortex lattice.

Similar studies have been performed for the superfluid Helium ^{3}He phase. The authors in ref. [19] have measured the superfluid acoustic impedance of ^{3}He-B coated with a wall of several layers of ^{4}He. The measurement has been performed using the resonance frequency of an ac-cut transducer which oscillates in a shear or longitudinal mode. The coating was used to enhance the specularity of quasi-particle scattering by the wall. In our case we do not have a rough wall and do not approximate the scattering by quasi-classical theory with a random S-matrix. Instead, we use an oscillating wall and compute the dissipative viscosity using the linear response theory given by Equations (14)-(18). We make use of the full spectrum of the zero and non-zero modes given in Equations (5)-(11).

a) Impedance for non-zero modes

The dissipative quasi-particle contribution $\zeta^{(R)}_{22,01}(\boldsymbol{Q},\Omega;qp)$ in the absence of Majorana modes is:

$$\zeta^{(R)}_{22,01}(\boldsymbol{Q},\Omega;qp)\equiv\frac{\Delta}{2k_0}Q_1Q_2\sum_{n_1}\sum_{n_2}\left[\frac{1}{\mathrm{e}^{\frac{E(n_1,n_2)}{T}}+1}-\frac{1}{\mathrm{e}^{\frac{E\left(n_1,n_2-\frac{Q_2d}{2\pi}\right)}{T}}+1}\right]$$
$$\times\left(\frac{-i}{\Omega}\right)\left[\frac{1}{i\hat{\Gamma}+\Omega+E(n_1,n_2)-E\left(n_1,n_2-\frac{Q_2d}{2\pi}\right)}-\frac{1}{i\hat{\Gamma}+\Omega-E(n_1,n_2)+E\left(n_1,n_2-\frac{Q_2d}{2\pi}\right)}\right].\tag{24}$$

In this subsection the superscript $(\neq 0,0)$ is implicit in the expression for $\zeta^{(R)}_{22,01}$. Here Δ is the TS pairing field, $q=\frac{2\pi}{d}$ is the momentum of the vortex lattice with the vortex separation distance d, Ω is the frequency of the applied strain field and $\hat{\Gamma}$ is the scattering life-time. We find $\zeta^{(R)}_{22,01}(\boldsymbol{Q},\Omega;qp)\approx\frac{\Delta}{2k_0}Q_1Q_2\cdot10^5 I_{qp}(t)\left[\mathrm{Newton}\cdot\mathrm{sec}/\mathrm{m}^3\right]$.

The gap parameter $\frac{\Delta}{2k_0}$ controls the dissipative stress. Using Equation (24) with the gap parameter $\frac{\Delta}{2k_0} q n_{\max} \approx 0.1\,\text{meV}$, momentum $q = 10^8\ \text{m}^{-1}$, and vortex lattice $d = 10^{-7}\ \text{m}$ we have $\frac{\Delta}{2k_0} \approx 10^{-31}\ \text{Joule}\cdot\text{m}$ and find:

$\zeta^{(R)}_{22,01}(\mathbf{Q},\Omega;qp) \approx \frac{Q_1}{q}\frac{Q_2}{q} q^2 \times 10^{-31} \times 10^5 I_{qp}\left[\text{Newton}\cdot\text{sec/m}^3\right] = \frac{Q_1}{q}\frac{Q_2}{q} 10^{-10} I_{qp}$ $\left[\text{Newton}\cdot\text{sec/m}^3\right]$, with $I_{qp}(t)$ varying from 1 to 6.

Figure 1 shows that the sound dissipative impedance is controlled by the absorption edge condition $\epsilon(b,k_F) > t$ [here t is the temperature and $\epsilon(b,k_F)$ is the ground state energy determined by the magnetic field *b*]. Using the explicit formula $\epsilon(b,k_F) = \epsilon_0(b,k_F) - \frac{v}{2k_F} k_F^2 \equiv \frac{vk_F}{2}\left(\frac{1}{2\pi}\frac{q^2}{k_F^2} - 1\right)$, $\epsilon_0(b,k_F) = \frac{vk_F}{2}\sqrt{\frac{b^2}{2}}$ given in Equation (11) we can determine from the impedance $\zeta^{(R)}_{22,01}(\mathbf{Q},\Omega;qp)$ the magnetic field b and the vortex lattice constant *d*.

The absorption is given in units of $\text{Newton}\cdot\text{sec/m}^3$. We plot $\frac{\zeta^{(R)}_{22,01}(\mathbf{Q},\Omega;qp)}{10^{-10}}$ for the case $\Delta = 0.1\,\text{meV}$ and $\Omega = 2\pi\times10^6\ \text{radians/sec}$ as a function of temperature t ($t = 0.1\,\text{meV}$ corresponds to 1 Kelvin) and the vortex separation is $d = 10^{-7}\ \text{m}$. The function $I_{qp}(t)$ is shown for three different cases: The *thin line* gives the absorption for the ground state energy $\epsilon(b,k_F) \equiv \frac{vk_F}{2}\left(\frac{q^2}{8\pi k_F^2} - 1\right) = 0.001\,\text{meV}$, the *thickest line* represents the absorption for the ground state energy $\epsilon(b,k_F) = 0.1\,\text{meV}$. The *line in between* describes

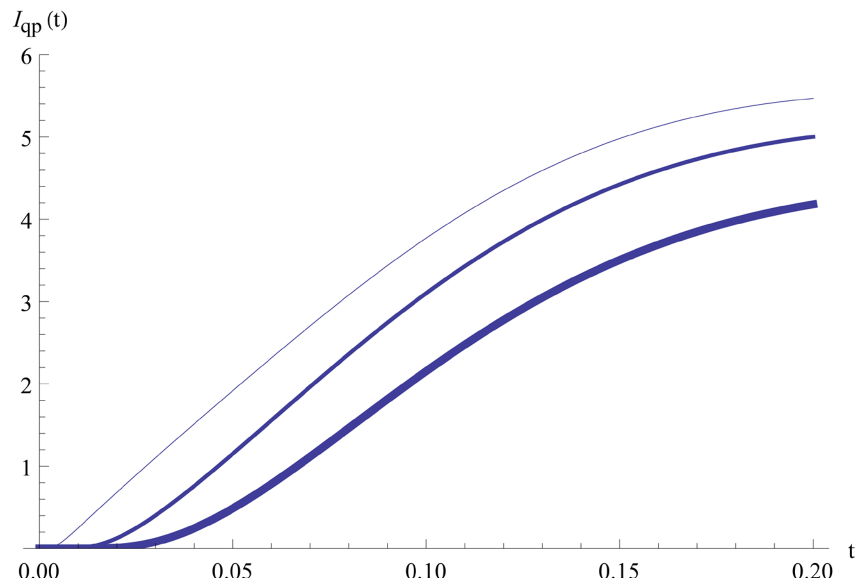

Figure 1. The dissipative part for the particle-hole contribution, $\frac{\zeta^{(R)}_{22,01}(\mathbf{Q},\Omega;qp)}{10^{-10}} \approx \left(\frac{Q_1}{q}\right)\left(\frac{Q_2}{q}\right) I_{qp}(t)\left[\text{Newton}\cdot\text{sec/m}^3\right]$, with only $I_{qp}(t)$ shown here.

the situation for $\epsilon(b,k_F)=0.0075\,\text{meV}$. We observe that the absorption edge temperature scales with the energy $\epsilon(b,k_F)$ as a function of the magnetic field and Fermi energy.

b) Impedance for Majorana modes

The Majorana contribution given by the particle-hole [see Equation (21)] depends on the tunneling amplitude t_0. We consider the ground state energies $\epsilon(b,k_F)=0.005\,\text{meV}$ (thin line), $\epsilon(b,k_F)=0.1\,\text{meV}$ (thick line) and $\epsilon(b,k_F)=0.05\,\text{meV}$ (intermediate ground state energy).

The Majorana contribution for the particle-particle part [see Equation (22)] for the same values of $\epsilon(b,k_F)$ and tunneling amplitude t_0 as in Figure 2 shows an absorption for low temperatures. Comparing Figure 1 with Figure 2, Figure 3 we observe that the Majorana fermion gives rise to absorption at low temperatures, in a region where the particle-hole absorption (Figure 1) is absent.

Since impurities are always present, it is important to know how to differentiate between the impurity absorption and the Majorana fermions. Impurities will give rise to absorption for frequencies $\Omega>\epsilon(b,k_F)-\epsilon_{\text{impurity}}$ and for temperatures $T>\Omega$; on the other hand, the Majorana absorption persists at $T\to 0$ (see Figure 3). The total impedance is given by the sum of contributions in the three Figures 1-3. We therefore conclude that the information about the Majorana modes, the magnetic field and tunneling amplitude t_0 can be obtained from the viscosity stress measurement.

7. The Sound Wave Analog of Andreev Crossed Reflection

Next we comment on the sound wave analog of the Andreev reflection. Two

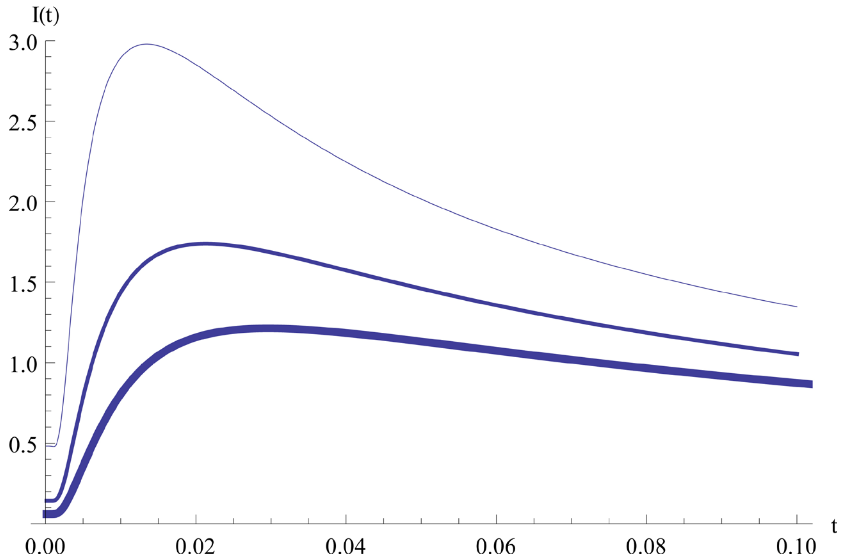

Figure 2. The dissipative impedance for Majorana particle-hole contribution $\frac{\zeta^{\neq 0,0}_{22,01}(\mathbf{Q},\Omega;qp)}{10^{-10}}\approx\left(\frac{Q_1}{q}\right)\left(\frac{Q_2}{q}\right)10^{-2}I(t)\left[\text{Newton}\cdot\text{sec}/\text{m}^3\right]$, with only $I(t)$ shown here. The range of temperature is $0.005<t<0.1$ (temperature $t=1$ corresponds to 0.1 meV and the structure for $t<0.005$ is an artifact of the numerics).

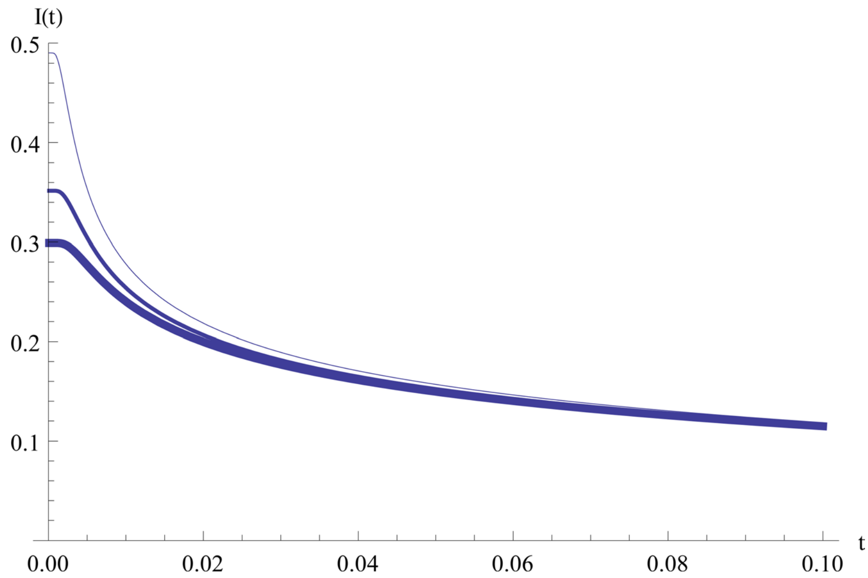

Figure 3. The dissipative impedance for Majorana particle contribution $\frac{\zeta^{\neq 0,0}_{22,22}(\mathbf{Q},\Omega;pp)}{10^{-10}} \approx \left(\frac{Q_1}{q}\right)\left(\frac{Q_2}{q}\right)10^{-1}I(t)\left[\text{Newton}\cdot\text{sec/m}^3\right]$ as a function of $\epsilon(b,k_F)=0.005\ \text{meV}$ (thin line), $\epsilon(b,k_F)=0.0075\ \text{meV}$, $\epsilon(b,k_F)=0.01\ \text{meV}$ (thick line). Only $I(t)$ is shown here. The range of temperature is $0.005<t<0.1$ (temperature $t=1$ corresponds to 0.1 meV and the structure for $t<0.005$ is an artifact of the numerics).

Majorana modes located at the two ends of a *p*-wave superconductor wire are detectable by piezoelectric transducers representing the sound equivalent of the two-leads experiments which measure the Andreev crossed reflection [40] [41]. We demonstrate that the same equations which were obtained for the Andreev crossed reflection [40] [41] induced by a voltage between the two tips are obtained for a sound wave which creates a time-dependent lattice deformation $D(t)=u\left(\frac{L}{2},t\right)+u\left(-\frac{L}{2},t\right)$. Here $u\left(\pm\frac{L}{2},t\right)$ is the sound deformation in the vicinity of each tip. The lattice deformation acts as a bias field. The voltage field $\mathrm{e}^{\pm i\frac{e}{\hbar}Vt}$ in the two-tip experiment is replaced by a bias field $\mathrm{e}^{\pm ik_F D(t)}$ for the sound wave case.

We follow the derivation given in refs. [40] [41]. For a *p*-wave (or equivalently a one-dimensional wire with spin-orbit interaction in the proximity of an *s*-wave superconductor and a magnetic field) with length L we have two Majorana modes localized at $x=-\frac{L}{2}$ and $x=\frac{L}{2}$. The fermions for the two tips are represented by $C_1\left(x=-\frac{L}{2}\right)=\mathrm{e}^{ik_F\left(-\frac{L}{2}\right)}R_1\left(x=-\frac{L}{2}\right)+\mathrm{e}^{-ik_F\left(-\frac{L}{2}\right)}L_1\left(x=-\frac{L}{2}\right)$ and $C_2\left(x=\frac{L}{2}\right)=\mathrm{e}^{ik_F\left(\frac{L}{2}\right)}R_2\left(x=\frac{L}{2}\right)+\mathrm{e}^{-ik_F\left(\frac{L}{2}\right)}L_2\left(x=\frac{L}{2}\right)$. (Here R_1, R_2, L_1 and L_2 are the right and left chiral fermions and k_F is the Fermi momentum of the electrons).

Following ref. [41] we integrate the Majorana fermions and obtain the coupling between the two tips: $H_{eff}(t)=(-ig^2)\int_0^\infty \mathrm{d}\tau\chi^+(t)\mathrm{e}^{-i\epsilon_0\tau}\chi(t-\tau)$ where ϵ_0 is the overlap energy between the two Majoranas. Ignoring the oscillating terms $\mathrm{e}^{ik_F\left(\pm\frac{L}{2}\right)}$ allows us to simplify the form of H_{eff}. In order to study the response to sound waves we replace $\mathrm{e}^{\pm ik_F\left(\pm\frac{L}{2}\right)}\to\mathrm{e}^{\pm ik_F\left(\pm\frac{L}{2}+u\left(\pm\frac{L}{2}\right)\right)}$, where $u\left(\pm\frac{L}{2}\right)$ is the sound deformation induced by the transducer. The deformation field $D(t)=u\left(\frac{L}{2},t\right)+u\left(-\frac{L}{2},t\right)$ is a function of the transducer frequency Ω. The velocity strain field is given by $\epsilon_{01}(t)=\partial_t D(t)$. The derivative of the effective Hamiltonian $H_{eff}(t)$ with respect to the strain velocity $\epsilon_{01}(t)$ determines the momentum density $\pi(x,t)$,

$$\pi(x,t)=\frac{\partial H_{eff}(t)}{\partial(\partial_t D(t))}\approx\left(\frac{-ig^2k_F}{\epsilon_0}\right)\theta[t]\left[\mathrm{e}^{ik_F D(t)}J\left(-\frac{L}{2},\frac{L}{2};t\right)+\mathrm{e}^{-ik_F D(t)}J^*\left(-\frac{L}{2},\frac{L}{2};t\right)\right]$$

where

$$\begin{aligned}J\left(-\frac{L}{2},\frac{L}{2};t\right)\equiv{}&L_2^\dagger\left(\frac{L}{2},t\right)R_1\left(-\frac{L}{2},t\right)-L_1^\dagger\left(-\frac{L}{2},t\right)R_2\left(\frac{L}{2},t\right)\\&+R_1\left(-\frac{L}{2},t\right)R_2\left(\frac{L}{2},t\right)\\&+L_2^\dagger\left(\frac{L}{2},t\right)L_1^\dagger\left(-\frac{L}{2},t\right).\end{aligned}$$

Here $J\left(-\frac{L}{2},\frac{L}{2};t\right)$ is the correlation between the tips; when a voltage is applied between the tips this correlation represents the current operator [41].

From the momentum density we compute the dissipative viscosity and the time ordered correlation function, $R_{01,01}(q,\Omega)=\left(\frac{-i}{\hbar}\right)\left\langle\left|T\left(\pi(q,t)\pi(-q,0)\right)\right|\right\rangle$. Following Equation (18) we obtain the viscosity $\zeta_{01,01}(q,\Omega)=-\frac{R_{01,01}(q,\Omega)}{i\Omega}$. The viscosity $\zeta_{01,01}(q,\Omega)$ is equivalent to the Andreev crossed reflection conductance obtained when voltage is applied between the tips [40] [41]. [To compare the two correlation functions we need to replace $\frac{e}{\hbar}Vt$ with $k_F D(t)$ and g^2e with $\frac{g^2k_F}{\epsilon_0}$.]

8. The Dissipative Superfluid Flow through Solid ^{4}He

The series of experiments performed by [20] show a flow of a superfluid through solid ^{4}He. Our starting point is the model for solid Helium in the broken symmetry phase including phonons $\boldsymbol{u}(\boldsymbol{x},t)$ and localized quasiparticles $\Psi(\boldsymbol{x},t)$ pinned by the solid:

$$S=\int \mathrm{d}t\int \mathrm{d}^3x\Big[\Psi^{\dagger}(\boldsymbol{x},t)i\partial_t\Psi(\boldsymbol{x},t)-\mu_{eff}(T)\Psi^{\dagger}(\boldsymbol{x},t)\Psi(\boldsymbol{x},t)+\gamma(T)\left|\nabla\Psi(\boldsymbol{x},t)\right|^2$$
$$+G(T)\left(\Psi^{\dagger}(\boldsymbol{x},t)\Psi(\boldsymbol{x},t)\right)^2-\Psi^{\dagger}(\boldsymbol{x},t)\Psi(\boldsymbol{x},t)\left|\rho_l(\boldsymbol{x},t)\right|\cos\left[\boldsymbol{b}_l\cdot\boldsymbol{u}(\boldsymbol{x},t)\right]$$
$$+\frac{1}{2}\left(\partial_t u^i\right)^2+\tilde{\mu}_{eff}(T)\left(\partial_i u^j\right)^2+\frac{\lambda(T)}{6}\left(\partial_i u^i\right)^2\Big].$$

We propose to explain the experiment [20] by applying two principles introduced in this paper : a-The coordinate transformation, b-The identification of the analog of the Majorana modes. We consider a model with two leads connected to a superfluid reservoirs which are described in the Bosonic language of a Luttinger liquid. The Majorana tunneling term is identify with the low energy bosons confined around the dislocation.(The low energy excitation is the analog of the Majorana). Around the dislocation the bosons are free to move in a direction perpendicular to the two-dimensional plane of the dislocations [32]. The bosons are disordered in the vicinity of the dislocation line. Due to the bending of the dislocation line the bosons binding energy depends on the local curvature. As a result we have a situation where the superfluid reservoirs are coupled to low energy excitations; due to the varying curvature they can be treated as disordered bosons (the density waves will not contribute, due to the large energy needed to excite regular bosons).

First we need to understand the effect of the coordinate transformation: In an ideal crystal the low momentum will give rise to the quasi particles excitations, the momentum corresponding to the inverse lattice separation will give rise to the density wave crystal Hamiltonian with the periodicity $\boldsymbol{u}(x,t)=\boldsymbol{u}(\boldsymbol{x}+\boldsymbol{R},t)$ ($\boldsymbol{R}$ is the crystal periodicity). A supersolid is not formed since the low energy quasi-particles are pinned by the mass of the density excitations. The coupling between the density excitation and the low energy quasi-particles is given by:

$$\Psi^{\dagger}(\boldsymbol{x},t)\Psi(\boldsymbol{x},t)\left|\rho_l(\boldsymbol{x},t)\right|\cos\left[\boldsymbol{b}_l\cdot\boldsymbol{u}(\boldsymbol{x},t)\right]\approx\Psi_0^{\dagger}(\boldsymbol{x},t)\Psi_0(\boldsymbol{x},t)\left|\rho_l(\boldsymbol{x},t)\right|$$

Here $\boldsymbol{b}_l$ is the reciprocal lattice vector and $\boldsymbol{u}(\boldsymbol{x},t)$ are the phonons. $\left|\rho_l\right|$ is the bosonic density which provides the large pinning mass and prevents the exitations of the quasiparticles. In the *vicinity* of an edge dislocation the term $\cos\left[\boldsymbol{b}_l\cdot\boldsymbol{u}(\boldsymbol{x},t)\right]$ vanishes. To see this consider an edge dislocation at $x=0$: $\xi^1=x$, $\xi^2=y-\frac{B^2}{2\pi}\tan^{-1}\frac{x}{y}$, $\xi^3=z$, where B^2 is the Burgers vector. Performing a spatial integration with respect y in thevecinity of the dislocation we find:

$$\int_{-b}^{b}\mathrm{d}y\cos\left[b_1\frac{B^2}{2\pi}\frac{y}{x^2+y^2}u^1(\boldsymbol{x},t)+b_2\left(1-\frac{B^2}{2\pi}\frac{y}{x^2+y^2}\right)u^2(\boldsymbol{x},t)+b_3u^3(\boldsymbol{x},t)\right]\Bigg|_{x=0}\approx 0$$

As result we have:

$$\Psi^{\dagger}(\boldsymbol{x},t)\Psi(\boldsymbol{x},t)\left|\rho_l(\boldsymbol{x},t)\right|\cos\left[\boldsymbol{b}_l\cdot\boldsymbol{u}(\boldsymbol{x},t)\right]\Big|_{x=0}\approx 0$$

The dislocation causes the replacement of the kinetic energy

$\left|\nabla\Psi_0(\boldsymbol{r},t)\right|^2 \to g^{i,j}\Psi^{\dagger}(\boldsymbol{r},t)\partial_i\partial_j\Psi(\boldsymbol{r},t)$ where $g^{i,j}$ is the metric tensor introduced by the edge dislocation. In the *z* direction the metric tensor is $g^{3,3}=1$. As a result the crystal has low energy excitations $\Psi_0(\boldsymbol{r}=z)$ in the *z* direction. For a finite density of dislocations we will have a direction perpendicular to the surface of the dislocations where quasi particles can propagate. For each dislocation $\alpha(s)$ we will have one dimensional low energy solution $\Psi_0(\alpha(s))$. Since the path $\alpha(s)$ is not a straight line the curvature of the dislocation line gives rise to bound states (realistic modeling of the free path boson is waveguide tube with a narrow width around the dislocation). The distribution of the curvature for different line dislocations can be considered as a source of disorder. As a result the model of the solid is restricted to the low energy paths. The paths which are not dislocations have high resistivity. Since the paths are in parallel we can neglect high resistivity paths. The conducting pats of the solid is given by, $S^{(\text{solid})}=\sum_{\alpha=1}S_\alpha$ (to treat exactly the disorder we need to use the replicas trick). Restricting ourselves to the free bosons confined to the dislocations line we have:

$$S^{\alpha(s)} \approx \int \mathrm{d}t \int \mathrm{d}s \left[\frac{1}{2vK_0}\left(\partial_t\Phi(s,t)\right)^2 - \frac{v}{2K_0}\left(\partial_s\Phi(s,t)\right)^2 + g(s)\cos\left[\Phi(s,t)\right]\right], \quad (25)$$

where $g(s)$ is a randomly distributed variable, due to the random curvature. The model for the superfluid reservoirs S_L and S_R is:
$S_L=\int \mathrm{d}t \int \mathrm{d}s\left[\frac{1}{2vK}\left(\partial_t\Theta_L(x,t)\right)^2-\frac{v}{2K}\left(\partial_x\Theta_L(x,t)\right)^2-\mu_L\partial_x\Theta_L(x,t)\right]$. For the right reservoir we have S_R with $\Theta_L(x,t)$ replaced by $\Theta_R(x,t)$ and chemical potential $\mu_L \neq \mu_R$.

The coupling between the low energy excitations and the two reservoirs is:

$$\begin{aligned} H_t = \int \mathrm{d}s \Bigg[& t_L \cos\left[\sqrt{4\pi}\left(\Theta_L\left(x\approx -\frac{L}{2},t\right)-\Phi\left(s=-\frac{L}{2},t\right)\right)\right] \\ & + t_R \cos\left[\sqrt{4\pi}\left(\Theta_R\left(x\approx \frac{L}{2},t\right)-\Phi\left(s=\frac{L}{2},t\right)\right)\right]\Bigg] \end{aligned}.$$

The disipative flow is given by a similar formula to the formula for the Andreev tunneling. The wires are replaced by the reservoirs and Majorana tunneling Hamiltonian by the tunneling of through the path caused by dislocations. As a result we propose the viscosity tensor given by the correlation of the two reservoirs superfluids which tunnels through the solid:

$$R_{11,11}(x,x',t-t')=\left(\frac{-i}{\hbar}\right)\left\langle G_0\right|\mathbf{T}\left(\Sigma_{11}^{R}(x,t)\Sigma_{11}^{L}(x',t')\mathrm{e}^{\frac{-i}{\hbar}\int_{-\infty}^{\infty}\mathrm{d}t'' H_t(t'')}\right)\left|G_0\right\rangle.$$

Here G_0 is the ground state in the absence of the tunneling Hamiltonian H_t.

The quantity $R_{11,11}(x,x',t-t')$ is to comparable with with the Hallock experimental results discussed by [20].

9. Conclusion

In the first part of this paper, we derived the spinor solution for an Abrikosov vortex lattice in a topological superconductor. We then obtained the zero and non-zero mode wave functions. These results have been used to compute the dissipative viscosity, which is obtained as a stress response to an applied velocity strain field. Experimentally one uses two transducers, one for measuring the stress response and the second transducer to generate the strain field. We find in addition to the particle-hole contribution, a viscosity term which reflects the presence of Majorana fermions. In the second part, we analyse the dissipative flow through Probing the p-wave wire with a sound wave one thus finds an effect similar to the Andreev crossed reflection. In last part, we consider the dissipative superfluid flow through solid ^{4}He. We show that the dislocation forms an effective one dimensional zero mode.

References

[1] Fu, L. and Kane, C.L. (2009) *Physical Review Letters*, **102**, Article ID: 216403. https://doi.org/10.1103/PhysRevLett.102.216403

[2] Potter, A.C. and Lee, P.A. (2011) *Physical Review B*, **83**, Article ID: 184520. https://doi.org/10.1103/PhysRevB.83.184520

[3] Xu, J.P., Liu, C., Wang, M.X., Ge, J., Liu, Z.L., Yang, X., Chen, Y., Liu, Y., Xu, Z.A., Gao, C.L., Qian, D., Zhang, F.C. and Jia, J.F. (2014) *Physical Review Letters*, **112**, Article ID: 217001. https://doi.org/10.1103/PhysRevLett.112.217001

[4] Grosfeld, E. and Stern, A. (2006) *Physical Review B*, **73**, Article ID: 201303R. https://doi.org/10.1103/PhysRevB.73.201303

[5] Chiu, C.-K., Pikulin, D.I. and Franz, M. (2015) *Physical Review B*, **91**, Article ID: 165402. https://doi.org/10.1103/PhysRevB.91.165402

[6] Biswas, R.R. (2013) *Physical Review Letters*, **111**, Article ID: 136401. https://doi.org/10.1103/PhysRevLett.111.136401

[7] Aref, T., Delsing, P., Kockum, M.K., Gustafson, M.V., Johansson, G., Leek, P., Magnusson, E. and Manenti, R. (2015) Quantum Acoustics with Surface Acoustic Waves.

[8] Magnusson, E.B., Williams, B.H., Mannenti, R., Nerisisyan, M.-S., Peterrer, M.J., Ardavan, A. and Leek, P.J. (2015) *Applied Physics Letters*, **106**, Article ID: 063509. https://doi.org/10.1063/1.4908248

[9] Maali, A., Hurth, C., Boigard, R., Jai, C., Bouchacina, C. and Aime, J.-P. (2005) *Journal of Applied Physics*, **97**, Article ID: 074907. https://doi.org/10.1063/1.1873060

[10] Maynard, J.D. (1996) *Physics Today*, **49**, 26. https://doi.org/10.1063/1.881483

[11] Kadanoff, L. and Falko, I. (1964) *Physical Review*, **136**, A1170. https://doi.org/10.1103/PhysRev.136.A1170

[12] Tsuneto, T. (1961) *Physical Review*, **121**, 406.

[13] Kee, H.-Y., Kim, Y.B. and Maki, K. (2000) *Physical Review B*, **62**, 5877. https://doi.org/10.1103/PhysRevB.62.5877

[14] Schrieffer, J.R. (1964) Theory of Superconductivity. Benjamin, New York.

[15] Tinkham, M. (1996) Introduction to Superconductivity. Dover Publications, Mi-

neola.

[16] Philips, P. (2012) Advanced Solid State Physics. Cambridge University Press, Cambridge. https://doi.org/10.1017/CBO9781139031066

[17] Rodriguez, J.P. (1985) *Physical Review Letters*, **55**, 250. https://doi.org/10.1103/PhysRevLett.55.250

[18] Marenko, M.S., Bourbonnais, C. and Tremblay, A.M.S. (2004) *Physical Review B*, **72**, Article ID: 024508.

[19] Murakawa, S., Tamura, Y., Wada, Y., Wasai, M., Saitoh, M., Aoki, Y., Nomura, R., Okuda, Y., Nagato, Y., Yamamoto, M., Higashitani, S. and Nagai, K. (2009) *Physical Review Letters*, **103**, Article ID: 155301. https://doi.org/10.1103/PhysRevLett.103.155301

[20] Vechov, Y. and Hallock, R.B. (2014) *Physical Review B*, **90**, Article ID: 134511.

[21] Landau, L.D. and Lifshitz, E.M. (1959) Theory of Elasticity. Pergamon, Oxford.

[22] Landau, L.D. and Lifshitz, E.M. (1986) Fluid Mechanics. Pergamon, Oxford.

[23] Katanev, M.O. and Volovich, I.V. (1992) *Annals of Physics*, **216**, 1-28.

[24] Fetter, A.L. and Wallecka, J.D. (1971) Quantum Theory of Many-Particle Systems. Dover Publications. Mineola, New York.

[25] Ivanov, D.A. (2001) *Physical Review Letters*, **86**, 268. https://doi.org/10.1103/PhysRevLett.86.268

[26] Lutchyn, R.M., Nagornykh, P. and Yakovenko, V.M. (2008) *Physical Review B*, **77**, Article ID: 144516. https://doi.org/10.1103/PhysRevB.77.144516

[27] Bernevig, B.A. and Hughes, T.L. (2013) Topological Insulators and Superconductors. Princeton University Press, Princeton and Oxford. https://doi.org/10.1515/9781400846733

[28] Chamon, C., Jackiw, R., Nishida, Y., Pi, S.-Y. and Santos, L. (2010) *Physical Review B*, **81**, Article ID: 224515. https://doi.org/10.1103/PhysRevB.81.224515

[29] Abrikosov, A.A. (2004) *Reviews of Modern Physics*, **76**, 975. https://doi.org/10.1103/RevModPhys.76.975

[30] Read, N. and Green, D. (2000) *Physical Review B*, **61**, 10267. https://doi.org/10.1103/PhysRevB.61.10267

[31] Cheng, M., Lutchyn, R.M., Galitski, V. and Das Sarma, S. (2010) *Physical Review B*, **82**, Article ID: 094504. https://doi.org/10.1103/PhysRevB.82.094504

[32] Kosevich, A.M. (2005) The Crystal Lattice. Willey-VCH Verlag Gmbh and Co. GaA, Weinheim.

[33] Avron, J.E., Seiler, R. and Zograf, P.G. (1995) *Physical Review Letters*, **75**, 697. https://doi.org/10.1103/PhysRevLett.75.697

[34] Callen, H.B. (1990) Thermodynamics. John Wiley, New York.

[35] Bradly, B., Goldstein, M. and Read, N. (2012) *Physical Review B*, **86**, Article ID: 245309. https://doi.org/10.1103/PhysRevB.86.245309

[36] Geracie, M., Son, D.T., Wu, C. and Wu, S.-F. (2015) *Physical Review D*, **91**, Article ID: 045030. https://doi.org/10.1103/PhysRevD.91.045030

[37] Schmeltzer, D. (2014) *International Journal of Modern Physics B*, **28**, Article ID: 1450059. https://doi.org/10.1142/S0217979214500593

[38] Schmeltzer, D. (2015) Topological Insulators and Superconductors—A Curved Space Approach.

[39] Nakahara, M. (2003) Geometry, Topology and Physics. Taylor and Francis Group,

New York, London.

[40] Flensberg, K. (2010) *Physical Review B*, **82**, Article ID: 180516. https://doi.org/10.1103/PhysRevB.82.180516

[41] Schmeltzer, D. (2015) *Journal of Modern Physics*, **6**, 1371. https://doi.org/10.4236/jmp.2015.69142

Appendix: Invariance of the Hamiltonian under the Coordinate Transformation: Derivation of the Stress-Strain Hamiltonian

The viscosity tensor is obtained from the linear response of electrons in an external field [24]. In order to accomplish this task we need to identify the elastic analog of the external electromagnetic field. This is accomplished using the invariance of the action under the coordinate transformation.

The unperturbed crystal is described by the coordinates $\boldsymbol{x}$ and the deformed crystal by the coordinates $\boldsymbol{\xi}$. The distortion of the crystal is given by $\boldsymbol{u}$ which is caused either by the phonons of the crystal or by an external force. We use the system ξ^a to describe the orthonormal coordinates for the deformed crystal with the basis vector frame $\partial_{\xi^a}, a = 1,2,3$. The unperturbed crystal is described by the Cartesian coordinates x^i with the basis frame vectors $\partial_{x^i}, i = 1,2,3$. The two coordinate systems in the two frames are related [23]:

$$\boldsymbol{x} \to \boldsymbol{\xi}(\boldsymbol{x}) = \boldsymbol{x} + \boldsymbol{u}(\boldsymbol{\xi}),$$
$$\xi^a(\boldsymbol{x}) = x^a + u^a(\boldsymbol{\xi}),\ a = 1,2,3;\quad \xi^i(\boldsymbol{x}) = x^i + u^i(\boldsymbol{\xi}),\ i = 1,2,3, \tag{26}$$

where i represents the Cartesian coordinates and a represents the deformed crystal. When the deformation of the crystal $\boldsymbol{u}$ vanishes we have the relation $\boldsymbol{x} = \boldsymbol{\xi}$. This allows us to introduce the non-relativistic transformation of the derivatives:

$$\partial_{\xi^a} = \sum_{i=1,2,3} \frac{\partial x^i}{\partial_{\xi^a}} \partial_i = \sum_{i=1,2,3} \frac{\partial\left(\xi^i - u^i\right)}{\partial_{\xi^a}} \partial_i = \sum_{i=1,2,3} \left(\delta_{i,a} - \partial_a u^i\right)\partial_i;\ a = 1,2,3,$$
$$\frac{\mathrm{d}}{\mathrm{d}t} = \partial_t + \sum_{i=1,2,3} \partial_t u^i \partial_i. \tag{27}$$

The metric integration for the deformed space is given in terms of the crystal deformation vector field $\boldsymbol{u}$. That is, $\mathrm{d}t\mathrm{d}\xi^{a=1}\mathrm{d}\xi^{b=2}\mathrm{d}\xi^{c=3} = \mathrm{d}t\mathbf{e}\mathrm{d}x^1\mathrm{d}x^2\mathrm{d}x^3$, where $\mathbf{e}$ is the Jacobian of the coordinate transformation which for the two-dimensional case is given by: $\mathbf{e} = 1 - \left(\partial_1 u^1 + \partial_2 u^2\right) - \partial_1 u^1 \partial_2 u^2$. We replace $\partial_a u^j \approx \partial_i u^b \delta_{a,i} \delta_{j,b} \approx \partial_i u^j$ (the exact relation is given by the matrix equation $\sum_j \partial_a u^j \partial_j u^b = \delta_{a,b}$). We introduce the notation $\epsilon_{ij} = \frac{1}{2}\left(\partial_i u^j + \partial_j u^i\right)$, $\epsilon_{0i} = \partial_t u^i$ and $\Omega_{ij} = \frac{1}{2}\left(\partial_i u^j - \partial_j u^i\right)$. When the excitations are caused by the phonons, we use the phonon spectrum of the crystal (in the harmonic representation). Due to the compatibility conditions [32] we have $\Omega_{ij} = 0$ and for a crystal with disclinations we have $\Omega_{ij} \neq 0$.